RSC Advances

PAPER

View Article Online
View Journal | View Issue

Cite this: *RSC Adv.*, 2025, **15**, 19937

Optimizing waste valorization: catalytic co-pyrolysis of cabbage waste and tire waste for enhanced bio-oil and syngas production utilizing char as a reforming catalyst†

Mudassir Hussain Tahir, [a] Vikul Vasudev,[b] Muhammad Ibrahim,*[c] Modhi O. Alotaibi,[d] Fatima M. Abbas,[e] Tahani A. Y. Asseri[f] and Rana Muhammad Irfan[g]

This study explores the catalytic co-pyrolysis of cabbage waste (CW) and tire waste (TW) to enhance the yield and quality of bio-oil and syngas. Although CW is produced in large quantities from global cabbage cultivation, its lower hydrogen content limits its utility for fuel and chemical production. The co-pyrolysis process, utilizing char as a catalyst, presents a cost-effective approach to optimize product outputs by promoting the reforming of volatiles during thermal decomposition. Thermogravimetric-infrared spectrometry (TG-FTIR) and a dual-stage fixed bed reactor were employed to assess thermal behavior, the release of evolved gases and product composition. Results demonstrated that catalyst-assisted co-pyrolysis with char reduced non-condensable emissions to 33.45% and increased condensable products to 66.57%, compared to 39.57% and 60.46% for co-pyrolysis alone, and 49.23% and 50.77% for CW pyrolysis. Furthermore, char-mediated volatile reforming significantly decreased the oxygenated fraction to 6.7% from 13.6% in co-pyrolysis and 22.5% in CW pyrolysis and greatly increased phenolic compounds and aromatics to 28.3% and 31.7% from 22.3% and 27.8% for co-pyrolysis, 17.9% and 21.7% for biomass pyrolysis, respectively. This research highlights the potential of integrating biomass and waste materials to promote sustainable energy solutions through enhanced resource utilization and diminished environmental impact.

Received 20th May 2025
Accepted 6th June 2025

DOI: 10.1039/d5ra03554f

rsc.li/rsc-advances

1 Introduction

Biomass represents a unique renewable carbon source capable of conversion into solid, liquid, and gaseous fuels.[1] It holds significant potential for achieving zero and negative carbon emissions, making it a crucial component in climate change mitigation strategies and the pursuit of carbon neutrality.[2] The pyrolysis of renewable biomass to produce syngas with a self-regulated H/C molar ratio offers a viable alternative to traditional fossil fuels, such as coal, thereby supporting the chemical industry's demands. Biomass pyrolysis involves the thermal decomposition of macromolecular organic compounds in biomass, carried out under inert gas conditions. This process generates volatile compounds that include non-condensable gases like CO, H_2, CO_2, and CH_4, as well as condensable substances such as water, acids, hydrocarbons, and oxygenated compounds.[3] The solid residue consists of biochar and ash. Consequently, biomass pyrolysis not only produces high-quality syngas but also co-generates liquid bio-oil and solid biochar, both of which possess significant environmental and economic value with promising commercialization potential.[4]

Cabbage waste (CW) represents a significant potential feedstock for bio-oil and chemical production.[5] In light of global cabbage production reaching 71 million tons, approximately 30% of this crop is rendered as waste, thereby contributing to considerable environmental concerns.[6] Treatment methodologies for cabbage waste are evolving in response to increasingly stringent waste separation regulations.[5] Traditional methods such as landfilling, composting, and discharge into waterways are being supplanted by thermal treatment techniques.[7] Although fuel and chemicals derived from crop waste (CW) have gained research interest, CW's lower hydrogen content (4.23%)

[a]*Co-Innovation Center of Efficient Processing and Utilization of Forest Resources, College of Materials Science and Engineering, Nanjing Forestry University, Nanjing, 210037, PR China*

[b]*National-provincial Joint Engineering Research Center of Biomaterials for Machinery Package, Nanjing Forestry University, Nanjing 210037, China*

[c]*Department of Environmental Sciences, Government College University Faisalabad (38000), Pakistan. E-mail: ebrahem.m@gmail.com*

[d]*Department of Biology, College of Science, Princess Nourah bint Abdulrahman University, P. O. Box 84428, Riyadh, 11671, Saudi Arabia*

[e]*Applied College Dahran Al-Janoub, King Khalid University, Saudi Arabia*

[f]*Biology Department, College of Science, King Khalid University, Abha 61321, Saudi Arabia*

[g]*Department of Pharmacy, Shanghai jiao-tong University, 200240, China*

† Electronic supplementary information (ESI) available. See DOI: https://doi.org/10.1039/d5ra03554f

compared to other biomass sources such as *Acacia* (5.3%); Willow (5.76%) and Beech wood (5.42%);[8] Pine needles (7.08%);[9] Douglas fir (6.91%);[10] Corn cob (5.9%); Wheat straw (5.47%); Rice husk (6.34%);[11] Banana peel (5.67%);[12] Pea waste (5.60%);[13] Switchgrass (5.7%);[14] Pinewood sawdust (6.06%)[15] limits its potential for producing valuable fuel and chemicals.[16] Thus, its essential to find methods and approach to efficiently convert CW into alternative fuels. In anaerobic environments, biomass can be transformed into bio-oil, gas, and coke through pyrolysis, a valuable waste treatment method.[17,18]

Bio-oil, derived from conventional pyrolysis, serves as a substitute for traditional chemicals and petroleum-based fuels; however, it is characterized by high oxygen content, low stability, elevated acidity, and diminished calorific value, rendering it inferior to petroleum derivatives.[19,20] Research indicates that the co-pyrolysis of CW with tire waste (TW) improves the quality of pyrolytic products such as liquid and syngas. However, challenges concerning the oxygen content and elevated acidity remain prevalent.[21] In this study, we seek to investigate the catalytic co-pyrolysis of CW with TW. Catalysts in this context can be categorized into alkali salts, metal oxides, zeolites, and carbon-based catalysts. An evaluation of various types of catalysts reveals several obstacles that hinder their industrial applicability, including cost-effectiveness, accessibility of active sites, and issues surrounding coke deposition and recyclability.[22,23] Among transition metals, nickel (Ni) has demonstrated potential for reforming volatiles; however, its application is complicated by environmental toxicity concerns. Noble metals, while exhibiting superior catalytic efficiency, are largely constrained by their high costs.[24] Alkaline metals, such as sodium (Na), potassium (K), and lithium (Li), are effective catalysts but face challenges related to evaporation and recovery.[25,26]

In this context, carbon-based catalysts (CBCs), particularly char, have gained considerable attention due to their numerous advantages. Their advantages include abundance,[27] resistance to both acidic and basic conditions,[28] high thermal stability,[29] extensive surface areas,[30] and environmental friendliness.[31] Highlighting promising avenues for catalyst. Biochar, in particular, stands out as an effective support material due to its high specific surface area, which facilitates catalytic dispersion. Additionally, biochar's robust adsorption capacity supports tar decomposition and reforming processes, while naturally occurring alkali and alkaline earth metals (AAEMs) can catalyze volatile compounds, thus reducing oxygenates and enhancing product quality. These characteristics highlight promising avenues for the development and application of catalysts in the co-pyrolysis of CW and TW.[32] Char produced during pyrolysis exhibits multifunctional capabilities. Whether in its native state or following activation, both of which are classified as "carbon materials" it serves as a catalyst, provides active sites for inorganic components, and acts as a support medium.

However, single-stage pyrolysis, which involves the concurrent processing of feedstock and catalyst, presents challenges such as inadequate contact between volatiles and catalyst, which negatively impact product yields and hinder catalyst regeneration. To overcome these issues, a bifurcated approach called "pyro-reforming" has emerged, involving pyrolysis followed by the reforming of volatiles over a catalyst. This dual-stage process commences with the pyrolysis of waste materials, resulting in the production of pyrolytic volatiles and char. Subsequently, the volatiles undergo reforming within a catalytic reactor, yielding a liquid fraction composed of condensable products, commonly referred to as bio-oil. Notably, the char generated from the pyrolysis phase, whether in its native form or after activation, can function effectively as a catalyst for the reforming process, thereby highlighting the economic advantages of this approach. During the reforming stage, char significantly enhances heat utilization efficiency through two principal mechanisms: first, it exploits the latent heat associated with the vaporization of water *via* char gasification; second, it retains the sensible heat derived from both the volatiles and char, thereby optimizing overall thermal efficiency. Furthermore, char is enriched with alkali and alkaline-earth metal species, which possess catalytic properties that facilitate the reforming of volatiles. This catalytic activity, in conjunction with char's sacrificial role in reforming, further augments the efficacy of the entire process.[33]

2 The primary objectives of this study are to

(1) Investigate the co-pyrolysis behavior of hydrogen-deficient biomass in conjunction with hydrogen-rich waste using thermogravimetric analysis (TGA).

(2) Evaluate the impact of char catalyst on the relative concentration of evolved gases and the types of products generated; and

(3) Conduct gas chromatography-mass spectrometry (GC-MS) analysis of the bio-oil and syngas to assess its reforming quality and examine the role of char in enhancing process.

3 Materials and methods

3.1 Sample preparation

Cabbage waste (CW) was obtained from a local supplier in Suzhou, China. The preparation of CW involved drying at 105 °C for 24 hours to eliminate moisture, followed by grinding to a fine powder with a particle size of approximately 250 micrometers, using a 100-mesh screen. The dried CW was stored in a desiccator for subsequent experimental analysis. TW, serving as the plastic substrate, was sourced from Shanghai Plastic Technology Co., Ltd, with a particle size of less than 200 mesh (<0.16 mm). The ultimate analysis was conducted in accordance with ASTM D5373 standards, utilizing a LECO CHNS-932 analyzer, while proximate analysis followed ASTM protocols, with ash and volatile matter determined per ASTM D5142-09. The fixed carbon content was calculated by subtracting the sum of ash, moisture and volatile matter percentages from 100%. In the co-pyrolysis experiments, a biomass-to-plastic ratio of 1 : 1 was maintained.

3.2 Char preparation

A total of 100 grams of pre-prepared dry waste (CW : TW ratio of 1 : 1) was introduced into the pyrolysis reactor. The pyrolysis was conducted at a controlled temperature of 700 °C, with

a heating rate of 10 °C min^{-1}. The target temperature was maintained for 20 min, or until no further volatile emissions were detected. This process resulted in a yield of 28.7wt% char, which was subsequently used to reform the volatiles generated during pyrolysis or co-pyrolysis.

3.3 TGA and TG-FTIR analysis

Thermogravimetric analysis (TGA) was employed to investigate the decomposition behavior during pyrolysis. The TGA, coupled with Fourier Transform Infrared Spectroscopy (TG-FTIR), was conducted at a heating rate of 10 °C min^{-1}, utilizing nitrogen as the purge gas at a flow rate of 100 mL min^{-1}. Volatile gases generated during pyrolysis at 200 °C min^{-1} were analyzed with a Nicolet 50 FTIR spectrophotometer, with spectra recorded at a resolution of 4 cm^{-1} within the wavenumber range of 4000 to 600 cm^{-1}, comprising eight scans per sample. Gases were transferred from the TG analyzer to the FTIR gas cell *via* a heated transfer line, with the capillary bundle maintained at 260 °C to prevent gas liquefaction. The relative concentrations of the released gases were determined by integrating the peak areas in the FTIR spectra. According to distinct wavenumber of evolved gaseous products, CO_2 (2327 cm^{-1}), NO (1762 cm^{-1}), SO_2 (1342 cm^{-1}), CO (2279 cm^{-1}), (CH_3COOH (1653 cm^{-1}), H_2O (1450 cm^{-1}), C_6H_5OH (1287 cm^{-1}), HCOOH (1157 cm^{-1}) CH_3-CH_2OH (1063 cm^{-1}) and C=C (1537 cm^{-1}) were mainly detected during FTIR analysis.[34] The yields of chemical compounds generated during pyrolysis were evaluated utilizing the formulas presented in the ESI.†

3.4 Experiment of catalytic co-pyrolysis of CW and TW

Fig. 1 illustrates the catalytic pyrolysis of CW and TW within a two-stage fixed-bed reactor system. This process involves three key components: the carrier gas system, the two-stage reactor, and the condensation unit. The raw feedstocks and catalysts were precisely weighed and positioned in the upper layer, while the catalyst was placed in the lower layer, separated by quartz wool. The apparatus was assembled and assessed for gas tightness. Nitrogen (N_2) was employed as the carrier gas, supplied at a flow rate of 80 mL min^{-1} and purged for 20 min to remove residual air. Once the specified temperature in the catalyst section was reached, the upper layer was rapidly heated to 500 °C at a rate of 40 °C min^{-1}. The resulting volatiles passed through the catalyst layer and into the condensation unit, where the oil was collected for further analysis. All experiments were repeated in triplicate to ensure reproducibility. After terminating the N_2 flow, the condensation apparatus was rinsed with dichloromethane (DCM) and weighed to determine the mass and yield of the pyrolysis-derived oil. The oil samples were then separated and analyzed using the Shimadzu QP2010 Gas Chromatography-Mass Spectrometry (GC-MS) system, utilizing an Rtx-5Ms column (30 m length, 0.25 mm diameter, 0.25 μm thickness). The oven temperature was initially set to 50 °C for 2 min, followed by a ramp to 260 °C at a rate of 5 °C min^{-1}, maintaining this temperature for an additional 1 min. The total duration for separation was 45 min, with a split ratio of 100 : 1. Qualitative data analysis was performed using Shimadzu software, and product selectivity was calculated using the area normalization method.

Gas samples obtained from the experiment were analyzed using an Agilent 7820 A gas chromatograph (GC), outfitted with a 2 m molecular sieve and a 2 m packed column. Prior to each measurement, the GC was calibrated with a standard gas mixture comprising C_1, C_2, C_3 and C_4 hydrocarbons, CO, CO_2, and H_2, which facilitated the establishment of standard curves for these components. The temperature program for the

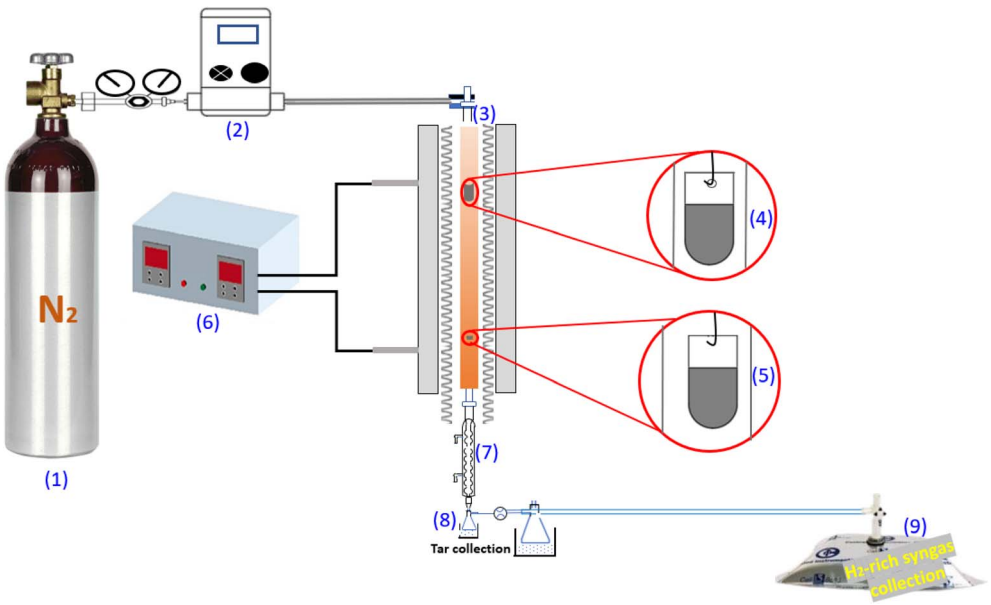

Fig. 1 Experimental setup for catalytic pyrolysis: (1) nitrogen cylinder; (2) mass flow meter; (3) tube furnace; (4) quartz crucible (containing sample); (5) quartz crucible (containing catalyst); (6) temperature controllers; (7) condenser pipe; (8) liquid nitrogen and ethanol mixture to collect oil; (9) gas bag for syngas collection.

detection process initiated at 50 °C for 22 min, followed by a ramp to 150 °C at a rate of 20 °C min^{-1}, and concluded with an increase to 230 °C at a rate of 50 °C min^{-1} for an additional 10 min. This methodology yielded comprehensive data on the composition and yield of the gas products.

The final yields of the pyrolysis products (liquid oil, char, and gas) were calculated by the following equations:

$$Y_o = (m_o \div m_i) \times 100 \quad (1)$$

$$Y_c = (m_c \div m_i) \times 100 \quad (2)$$

$$Y_g = 100\% - (Y_o \div Y_c) \quad (3)$$

where Y_o, Y_c, and Y_g are the yields of pyrolysis oil, char, and gas, m_o(g), and m_c(g) are the mass of pyrolysis oil and char, and m_i(g) is the initial mass of the sample.

4 Results and discussion

4.1 Materials characterization

Table 1 provides the ultimate and proximate analysis of coir waste (CW) and tree waste (TW) on a dry basis.

The results indicate that TW possesses a higher hydrogen content (10.03%), while CW exhibits a greater volatile matter content (73.61%) compared to other biomass sources, such as banana peel (66.79%),[35] rice husk (64%)[36] and walnut shell (63%).[37] The H/C and O/C atomic ratios for CW are 0.94 and 0.52, respectively. In contrast, TW demonstrates a higher hydrogen content, with an H/C ratio of 1.45 and a significantly lower O/C ratio of 0.04. These findings suggest that the co-pyrolysis of CW and TW may yield synergistic effects that enhance the quality of pyrolytic products. CW's low ash content (5.01%) is advantageous, as it reduces agglomeration and promotes thermal degradation.[38] Additionally, CW maintains a moisture content of 6.77%, below the 10% threshold necessary for industrial pyrolysis, facilitating the production of high-quality end products and improving energy efficiency.[34] The significant carbon content of CW (53.88%) indicates its potential for generating high-quality biochar suitable for catalytic applications.[39] Furthermore, the low nitrogen (2.01%) and sulfur (2.71%) levels in CW are environmentally beneficial, implying reduced emissions of harmful gases such as SO_x and NO_x during combustion. However, CW's relatively low hydrogen content (4.13%) as compared to reported biomasses (see Table 2) may limit its application in the production of bio-based chemicals and fuels, potentially resulting in increased emissions during thermochemical conversion processes.

Table 2 Comparison of hydrogen contents of cabbage waste with other biomasses reported

Biomass	H (wt%)	References
Cabbage waste	4.23	Present study
Rice husks	6.62	40
Oat straw	6.16	40
Olive husks	6.96	41
Pinewood	6.40	41
Willow, SRC	5.54	42
Banana peel	5.67	12
Pine bark	5.90	43
Wheat straw	6.11	43
Olive residue	6.82	42
Beech wood	5.42	8
Pine needles	7.08	9
Pinewood sawdust	6.06	15
Mango peel	5.17	39
Douglas fir	6.91	10
Pine sawdust	6.04	44
Twigs	5.88	45

To address this limitation, we propose the co-pyrolysis of CW with TW and the subsequent reforming of the volatiles using char produced from the co-pyrolysis process. This approach demonstrates cost-effectiveness and the potential for recyclability, thereby optimizing resource utilization.

4.2 Thermal behavior during pyrolysis, co-pyrolysis, and catalytic pyrolysis

Fig. 2a and (b) present the TGA and DTG curves for CW pyrolysis, TW pyrolysis, co-pyrolysis, and catalytic co-pyrolysis, performed at a heating rate of 10 °C min^{-1} and an inert gas (N_2) flow rate of 80 mL min^{-1}. The thermal degradation of CW occurs in three distinct phases. The initial phase (30–130 °C) is attributed to moisture loss.

The second phase (155–450 °C) encompasses the decomposition of hemicellulose, cellulose, starch, lignin, and proteins through various chemical reactions. The final phase (450–800 °C) relates to the pyrolysis of residual components.[46] The pyrolysis inflection point, indicating the maximum weight loss rate, is observed at 223.5 °C for CW, shifts to a higher temperature of 259.3 °C during TW co-pyrolysis, and decreases to 196.7 °C in catalytic co-pyrolysis. The primary peak during biomass pyrolysis reflects the thermal breakdown of hemicellulose and cellulose, while subsequent peaks pertain to lignin decomposition.[47] CW decomposition occurs within the temperature range of 182 to 326 °C, peaking at 229 °C, whereas TW exhibits

Table 1 Elemental and proximate analysis of CW and TW

	Proximate analysis (da, wt%)				Ultimate analysis (d, wt%)						
	M	A	V	FC	H	C	O	N	S	H/C	O/C
CW	6.77	5.01	73.61	14.71	4.23	53.88	37.17	2.01	2.71	0.94	0.52
TW	5.98	0.96	63.31	30.71	10.03	83.23	4.09	0.93	1.72	1.45	0.04

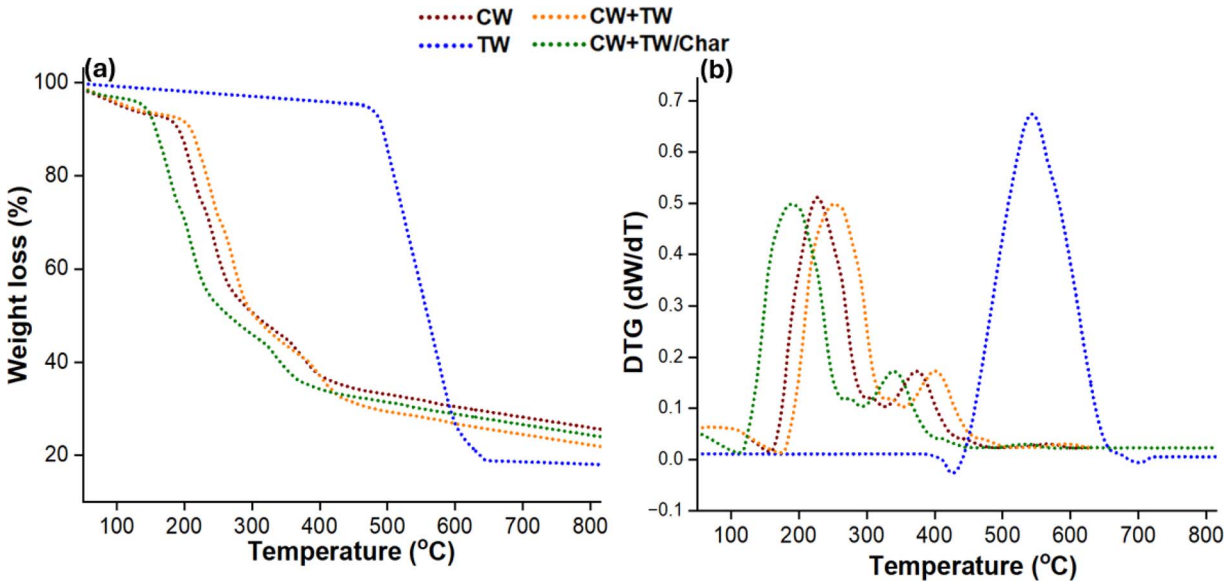

Fig. 2 (a) TGA and (b) DTG curves, for CW pyrolysis, TW pyrolysis, co-pyrolysis and catalytic co-pyrolysis (CW : TW = 1 : 1) with char as catalyst (feedstock to catalyst ratio = 2 : 1), using a 10 °C min^{-1} heating rate and 60 mL min^{-1} flow rate.

a decomposition range of 461 to 670 °C, with a peak at 553 °C. The DTG thermogram of TW demonstrates a prominent peak, denoting a single dominant reaction zone, which is indicative of its simpler monomeric structure and fewer chemical bond types. The degradation of synthetic polymers like TW typically follows a radical mechanism, primarily involving the cleavage or formation of radicals at C–H and C–C sigma bonds.[44] During co-pyrolysis, an increase in the inflection point suggests improved thermal stability.[48] TW begin thermal decomposition at higher temperatures (approximately 457 °C) due to the absence of inherent moisture, while biomass degrades at a considerably lower temperature (around 183 °C). The inflection point for biomass pyrolysis is noted at 229.5 °C, which shifts to 257.1 °C during co-pyrolysis, likely due to melting plastic encapsulating the biomass. This encapsulation impedes the release of volatiles during biomass pyrolysis, subsequently delaying thermal decomposition and increasing the inflection point. Biomass pyrolysis is primarily a radical-driven process leading to the formation of numerous small radical-containing molecules. These radicals tend to stabilize by reacting with those generated from plastic bond cleavage, which partially suppresses the radical polymerization originating from biomass, indicating a synergistic interaction between biomass and TW during co-pyrolysis.[49] Conversely, a reduction in the inflection points with catalyst addition, particularly with the incorporation of char, implies that the catalytic process lowers the energy barrier for forming the activated complex, thereby accelerating decomposition reactions and resulting in an earlier inflection point.[50]

4.3 TG-FTIR analysis

TG-FTIR analysis allows for the assessment of temperature variations and gas component emissions during the pyrolysis process.[51] However, due to the inherent complexity of gas mixtures and the limitations associated with FTIR, only select compounds can be reliably identified, omitting diatomic gases such as H2 and Cl_2.[52,53] The gaseous products evolved during pyrolysis comprise both condensable and non-condensable organic compounds. Notably, CO_2, NO, SO_2, and CO are classified as non-condensable gases; the remaining products are typically condensable.

FTIR spectral analysis conducted during the pyrolysis of CW, co-pyrolysis with TW, and catalytic co-pyrolysis with char is illustrated in Fig. S1.† The results indicate an inverse correlation between the yields of non-condensable and condensable gases, where an increase in one category corresponds to a decrease in the other. As illustrated in Fig. S2,† pyrolysis of CW resulted in a yield of condensable and non-condensable products at 50.77% and 49.23%, respectively. In contrast, co-pyrolysis with TW significantly reduced non-condensable products to 39.57% and increased condensable products to 60.46%. Catalyst-assisted co-pyrolysis with char further decreased non-condensable emissions to 33.45% while increasing condensable products to 66.57%. This underscores the potential of catalytic co-pyrolysis of hydrogen-deficient biomass, such as CW, with hydrogen-rich waste (TW) utilizing char as a catalyst for enhancing pyrolytic product yields. Condensable products generated through this process are amenable to subsequent purification and separation, whereas non-condensable gases pose environmental risks, contributing to pollution through emissions of SO_2 and NO. Fig. 3 presents the integral yields of condensable and non-condensable components.

The detection of alkenes and phenolic compounds in the condensable fraction emphasizes their potential for use in bioenergy and bio-based chemical applications. Importantly, compounds such as benzene and toluene, derived from alkenes, exhibit high heating values (49.9 and 41.8 MJ kg^{-1}) comparable to conventional fuels like gasoline and diesel (47.3 and 44.8 MJ

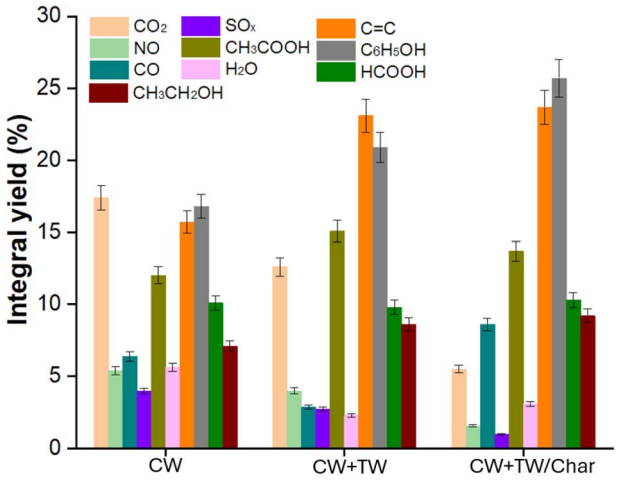

Fig. 3 Relative concentration of pyrolytic products of CW, co-pyrolysis with TW and catalytic pyrolysis with char at 500 °C.

kg^{-1}).[54] Phenolic derivatives have vast industrial applications, including chemical production, pharmaceuticals, colorants, and paper bleaching, as well as serving as herbicides and insecticides in agriculture.[55,56] Despite the benefits of these condensable products, the emissions of CO_2, CO, SO_2, and NO continue to pose significant environmental threats, contributing to the greenhouse effect. Notably, the co-pyrolysis of CW with TW and the catalytic co-pyrolysis process notably enhanced the relative concentrations of alkenes and phenols, peaking at 23.1% and 20.9% for co-pyrolysis, and 29.2% and 26.3% for catalytic co-pyrolysis, compared to 15.7% and 16.8% for non-catalytic pyrolysis. Conversely, the integral yields of pollutants such as CO_2, NO, CO, and SO_2 decreased to 2.73%, 8.6%, 2.86%, and 3.98%, respectively, in catalytic co-pyrolysis, in contrast to yields of 6.38% and 3.96% from pyrolysis alone. These findings suggest that catalytic co-pyrolysis of hydrogen-deficient biomass with char is a promising strategy to enhance product quality while mitigating emissions, benefiting advancements in bioenergy and biochemical sectors.

4.4 GC-MS analysis of bio-oil and syngas

Fig. 4a illustrate the yield (indicated by peak area) of bio-oil constituents obtained during the pyrolysis, co-pyrolysis, and catalytic reforming of volatiles derived from co-pyrolysis at a temperature of 500 °C. The results demonstrate that CW pyrolysis predominantly produces oxygenates and acids, with respective yields of 22.5% and 17.8%. In contrast, the yields of olefins, aromatics, phenols, and alcohols are significantly lower, recorded at 7.76%, 17.85%, 21.7%, and 8.6%. In the case of co-pyrolysis with TW, a noticeable decrease in the yields of oxygenates and acids to 13.7% and 8.2% is observed. Conversely, the yields of olefins, aromatics, phenols, and alcohols increase to 15.4%, 22.3%, 27.8%, and 12.1%, respectively. These findings suggest that co-pyrolysis effectively reduces the yield of oxygenates and acids while enhancing the production of value-added products, thereby significantly improving bio-oil quality. Further analysis of the catalytic reforming of volatiles produced from the co-pyrolysis of CW and TW reveals a substantial reduction in the yields of oxygenates and acids to 6.7% and 4.58%, respectively. Additionally, the yields of olefins, aromatics, and phenols are markedly enhanced to 23.7%, 28.3%, and 31.65%. This indicates the significant catalytic activity of char derived from co-pyrolysis, which contributes to the economic viability of the process. Fig. 4b presents the composition (vol%) of syngas generated during each process; pyrolysis, co-pyrolysis, and catalytic reforming of volatiles derived from co-pyrolysis at 500 °C. Notably, CW pyrolysis predominantly produces CO_2 and CO, with respective compositions of 38.7%, 18.6%, and 8.7%, alongside a H_2 composition of 23.7%. In the co-pyrolysis scenario, the yields of CO_2 and CO decrease to 28.5% and 15.3%, while the H_2 composition increases to 31.7%, indicating that co-pyrolysis effectively enhances H_2 yield in syngas. Furthermore, during the reforming of volatiles resulting from the co-pyrolysis of CW and TW (at a 1 : 1 ratio), the H_2 yield is further increased to 37.6%, while the yields of CO_2 and CO decrease to 22.7% and 12.5%. This underscores the significant catalytic activity of char in

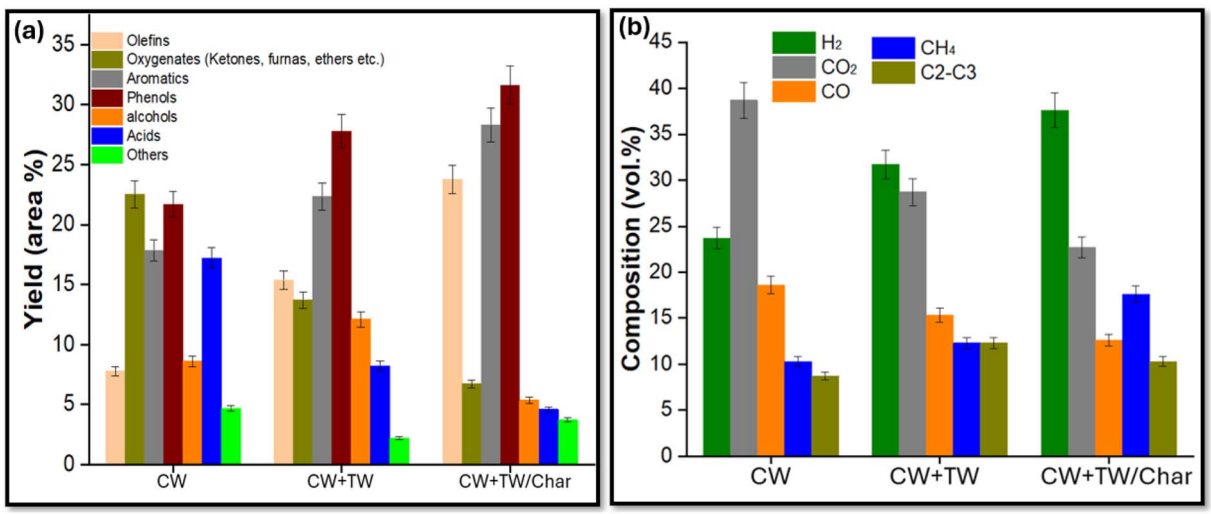

Fig. 4 (a) GCMS analysis of bio-oil and (b) syngas.

promoting a higher H_2 ratio in syngas, thereby demonstrating its potential for improving the efficiency of bio-oil conversion processes.

Enriching bio-oil with phenolic compounds is a strategic approach to enhance its economic value and sustainability within biorefineries. Recent studies indicate that catalytic co-pyrolysis of crop waste (CW) yields higher concentrations of phenolic compounds in the resultant bio-oil. This process thus presents a viable method for producing phenolic-rich bio-oil, which is of considerable interest for various applications. Aromatics, particularly benzene and toluene, are noteworthy for their high heating values (HHVs), recorded at 49.9 and 41.8 MJ kg^{-1}, respectively. These values are comparable to those of conventional fossil fuels, such as gasoline and diesel, which have HHVs of 47.3 and 44.8 MJ kg^{-1}, respectively. The increased aromatic content derived from catalytic co-pyrolysis significantly enhances bio-oil's potential as a bioenergy source, particularly in the form of aromatic-rich bio-oil. Furthermore, olefins such as propene, isoprene, D-limonene, and 2-methylpropene play essential roles across various industrial applications. For instance, D-limonene is commonly utilized in the production of pesticides, circuit boards, and as a dispersing agent for pigments. In summary, catalytic co-pyrolysis in conjunction with char optimizes the production of olefins from hydrogen-deficient crop waste, resulting in benefits for both the chemical and agricultural sectors. Moreover, ongoing research into the incorporation of hydrogen-rich syngas demonstrates significant potential for harnessing hydrogen from waste materials, thereby facilitating further energy applications. This dual focus on bio-oil enhancement and hydrogen recovery underscores the promising future of catalytic co-pyrolysis in advancing sustainable energy solutions.

4.5 Effect of reforming temperature

Higher temperatures are known to accelerate reaction rates, thereby increasing the production of chemical products. In the context of oil processing, it is observed that elevated temperatures enhance the production of aromatic compounds and phenols (Fig. 5a). However, the production of olefins tends to decrease, while the yields of oxygenates and acids fluctuate between 500 °C and 800 °C. In particular, oil samples with higher concentrations of aromatics and phenols were optimized at a temperature of 700 °C, where concentrations reached 32.6% and 34.8%, respectively. Beyond this temperature, further increases resulted in diminished content of these valuable compounds. Regarding the quality of syngas produced, the highest hydrogen yield was recorded at 900 °C, reaching 43.6%. In comparison, a slight yield of 42.8% was observed at 800 °C, indicating that this temperature may not significantly impact hydrogen production (Fig. 5b). Considering both the quality of oil and hydrogen production at a singular temperature, 800 °C is identified as the optimal temperature for reforming processes. This finding suggests a balance between maximizing product yields while maintaining the desired quality of both oil and hydrogen.

4.6 Mechanisms of biomass co-pyrolysis and the role of char as a catalyst in the reforming process

Fig. 6 illustrates the proposed mechanism of pyrolysis and the role of char as a reforming agent in the production of high-quality oil and syngas.

Biomass, upon undergoing decomposition, generates a diverse array of compounds. The process of co-pyrolysis facilitates the transfer of hydrogen to biomass-derived radicals, which is vital for deoxygenation. This transformation significantly improves the hydrogen-to-carbon effective ratio (H/C_{eff}), a crucial metric for evaluating production efficiency.[57] In the context of reforming volatile compounds, char serves as an efficient catalytic agent due to its high specific surface area. This characteristic provides a substantial interface for catalytic interactions. Furthermore, biochar possesses a considerable adsorptive capacity for tars, which aids in their thermal

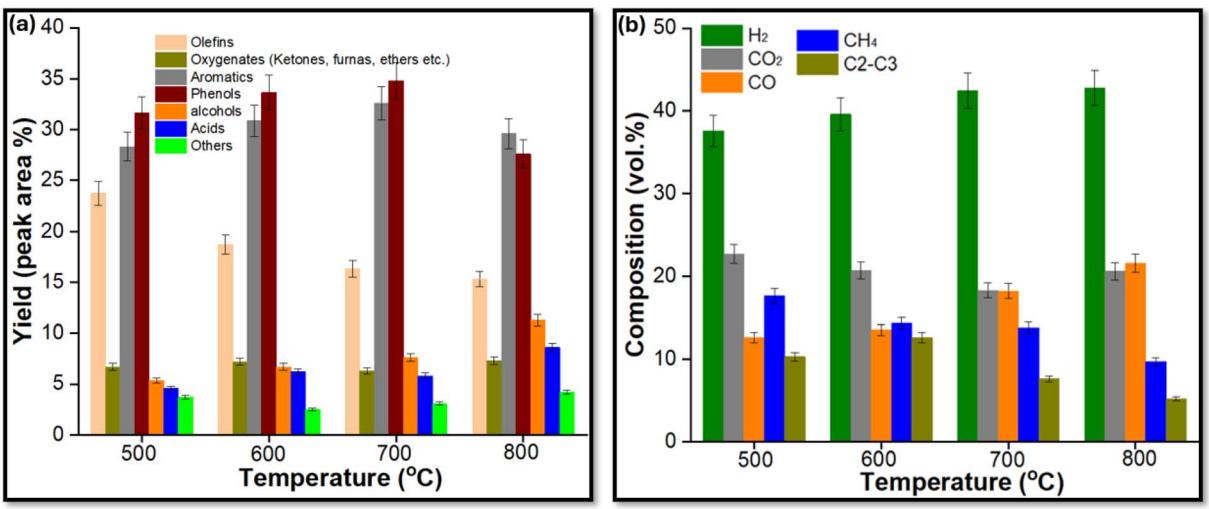

Fig. 5 Effect of reforming temperature on (a) oil products and (b) syngas composition.

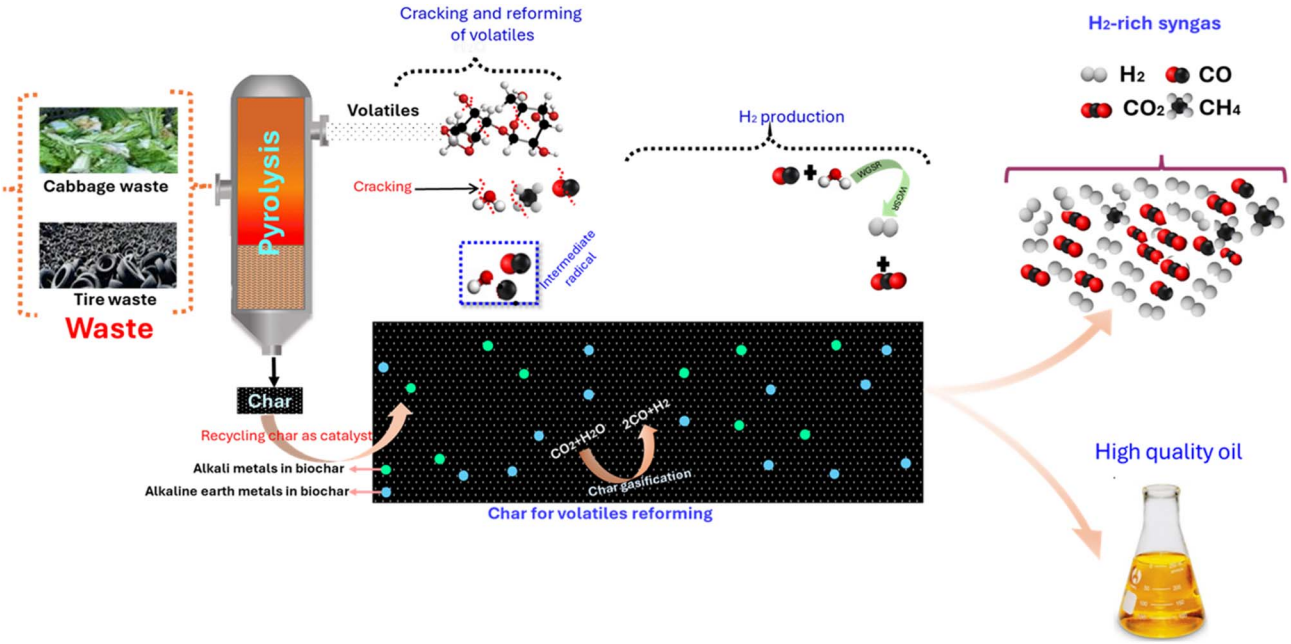

Fig. 6 The mechanisms underlying biomass co-pyrolysis and the function of char as a catalyst in the reforming process are critical areas of study.

breakdown. The char phase contributes to the cleavage and removal of oxygen from organic compounds through various reactions, including dehydration, decarbonylation, and decarboxylation.[58] Simultaneously, phenolic compounds undergo transformation, wherein unsaturated branches and methoxy groups are converted into olefins and smaller oxygenates.[59] These smaller oxygenates comprising ketones, aldehydes, furans, and phenols are subsequently adsorbed into the pores of char. Within this context, they undergo a series of reactions including dehydration, decarbonylation, decarboxylation, oligomerization, and aromatization.[60] Additionally, olefins can be further converted into aromatic hydrocarbons during these processes.[61] Moreover, the intrinsic presence of alkali and alkaline earth metals (AAEMs) in char catalyzes the water-gas shift (WGS) reaction, which plays a pivotal role in enhancing H_2 production. This catalytic activity is particularly significant during the reforming phase,[62], as it leads to increased production of H_2 and CO through the WGSR, while concurrently promoting yields of CO and methane through the Boudouard reaction and methanation processes. In conclusion, the processes of biomass co-pyrolysis and the catalytic role of biochar are crucial for optimizing the yield of valuable products, thereby enhancing the overall efficiency of biomass-derived energy systems.

5 Conclusion

In conclusion, this study demonstrates the effectiveness of catalytic co-pyrolysis of cabbage waste (CW) and tire waste (TW) in enhancing the yield and quality of bio-oil and syngas. The findings indicate that the co-pyrolysis approach leverages the synergistic interaction between hydrogen-deficient and hydrogen-rich feedstocks, resulting in improved thermal efficiency and favorable product profiles. Utilizing char as a catalyst in the dual-stage pyrolysis and reforming process increased the production of value-added products, including phenolic compounds and aromatics, with yields of 28.3 and 31.7 for char-assisted reforming, 22.3 and 27.8 for co-pyrolysis, and 17.9 and 21.7 for biomass pyrolysis. Additionally, the process mitigated the production of oxygenates, with yields of 22 for pyrolysis, 13.7 for co-pyrolysis, and 6.7 for char-assisted volatile reforming. Furthermore, optimizing operational parameters, particularly reforming temperature at 800 °C, enhances both bio-oil and hydrogen yield. This research contributes valuable insights into catalytic co-pyrolysis as a viable strategy for advancing the bioenergy sector and addressing environmental challenges associated with biomass waste. Future work should investigate the scalability and economic viability of this approach, along with a comprehensive life cycle assessment to evaluate overall sustainability.

Data availability

Data will be made available upon request.

Conflicts of interest

There is no conflicts to declare.

Acknowledgements

This work was supported by Princess Nourah bint Abdulrahman University Researchers Supporting Project number (PNURSP2025R101), Princess Nourah bint Abdulrahman University, Riyadh, Saudi Arabia. The authors extend their appreciation to the Deanship of Research and Graduate Studies

at King Khalid University for funding this work through Small Research Project under grant number RGP 1/43/46.

References

1 P. J. Megia, A. J. Vizcaino, J. A. Calles and A. Carrero, *Energy Fuels*, 2021, **35**, 16403–16415.
2 S. R. Paramati, U. Shahzad and B. Doğan, *Renewable Sustainable Energy Rev.*, 2022, **153**, 111735.
3 Y. Qureshi, U. Ali and F. Sher, *Appl. Therm. Eng.*, 2021, **190**, 116808.
4 T. M. I. Mahlia, N. Ismail, N. Hossain, A. S. Silitonga and A. H. Shamsuddin, *Environ. Sci. Pollut. Res.*, 2019, **26**, 14849–14866.
5 Y. Zhang, X. Cheng, Z. Wang, M. H. Tahir, Z. Wang, X. Wang and C. Wang, *Sci. Total Environ.*, 2022, **804**, 149951.
6 X. Zhang, H. Lei, S. Chen and J. Wu, *Green Chem.*, 2016, **18**, 4145–4169.
7 M. Sultana, M. Jahiruddin, M. R. Islam, M. M. Rahman and Md. A. Abedin, *Asian J. Soil Sci. Plant Nutr.*, 2020, 32–42.
8 C. E. Greenhalf, D. J. Nowakowski, A. B. Harms, J. O. Titiloye and A. V. Bridgwater, *Fuel*, 2013, **108**, 216–230.
9 A. K. Varma, N. Lal, A. K. Rathore, R. Katiyar, L. S. Thakur, R. Shankar and P. Mondal, *Energy*, 2021, **218**, 119404.
10 S. R. Wu, C. C. Chang, Y. H. Chang and H. P. Wan, *Fuel*, 2016, **175**, 57–63.
11 B. Biswas, N. Pandey, Y. Bisht, R. Singh, J. Kumar and T. Bhaskar, *Bioresour. Technol.*, 2017, **237**, 57–63.
12 M. H. Tahir, Z. Zhao, J. Ren, T. Rasool and S. R. Naqvi, *Biomass Bioenergy*, 2019, **122**, 193–201.
13 E. Müsellim, M. H. Tahir, M. S. Ahmad and S. Ceylan, *Appl. Therm. Eng.*, 2018, **137**, 54–61.
14 R. Conti, D. Fabbri, I. Vassura and L. Ferroni, *J. Anal. Appl. Pyrolysis*, 2016, **122**, 160–168.
15 E. Fernandez, L. Santamaria, M. Amutio, M. Artetxe, A. Arregi, G. Lopez, J. Bilbao and M. Olazar, *Energy*, 2022, **238**, 122053.
16 B. B. Uzoejinwa, X. He, S. Wang, A. El-Fatah Abomohra, Y. Hu and Q. Wang, *Energy Convers. Manage.*, 2018, **163**, 468–492.
17 S. Gupta, P. Mondal, V. B. Borugadda and A. K. Dalai, *Environ. Technol. Innovation*, 2021, **21**, 101276.
18 S. Zhong, B. Zhang, C. Liu, A. Shujaa aldeen, S. Mwenya and H. Zhang, *J. Anal. Appl. Pyrolysis*, 2022, **164**, 105544.
19 J. Alvarez, M. Amutio, G. Lopez, L. Santamaria, J. Bilbao and M. Olazar, *Waste Manage.*, 2019, **85**, 385–395.
20 M. S. Gad, H. Panchal and Ü. Ağbulut, *Energy*, 2022, **242**, 122945.
21 M. H. Tahir and N. Shimizu, *J. Anal. Appl. Pyrolysis*, 2023, **172**, 105992.
22 T. Jia, F. Zhou, H. Ma and Y. Zhang, *J. Anal. Appl. Pyrolysis*, 2021, **157**, 105217.
23 X. Xue, C. Zhang, D. Xia, Y. Wang, J. Liang and Y. Sun, *Chem. Eng. J.*, 2022, **431**, 134251.
24 G. Guan, M. Kaewpanha, X. Hao and A. Abudula, *Renewable Sustainable Energy Rev.*, 2016, **58**, 450–461.
25 K. Mitsuoka, S. Hayashi, H. Amano, K. Kayahara, E. Sasaoaka and M. A. Uddin, *Fuel Process. Technol.*, 2011, **92**, 26–31.
26 C. Hognon, C. Dupont, M. Grateau and F. Delrue, *Bioresour. Technol.*, 2014, **164**, 347–353.
27 H. H. Mardhiah, H. C. Ong, H. H. Masjuki, S. Lim and Y. L. Pang, *Energy Convers. Manage.*, 2017, **144**, 10–17.
28 L. J. Konwar, J. Boro and D. Deka, *Renewable Sustainable Energy Rev.*, 2014, **29**, 546–564.
29 Y. Pang, K. Luo, L. Tang, X. Li, J. Yu, J. Guo, Y. Liu, Z. Zhang, R. Yue and L. Li, *Environ. Sci. Pollut. Res.*, 2019, **26**, 32764–32776.
30 J. A. Sánchez, D. L. Hernández, J. A. Moreno, F. Mondragón and J. J. Fernández, *Appl. Catal., A*, 2011, **405**, 55–60.
31 H. Pan, Q. Xia, Y. Wang, Z. Shen, H. Huang, Z. Ge, X. Li, J. He, X. Wang, L. Li and Y. Wang, *Fuel Process. Technol.*, 2022, **237**, 107421.
32 W. Fan, M. H. Tahir, D. Chen, L. Hong, L. Yin and H. Yu, *J. Anal. Appl. Pyrolysis*, 2024, **178**, 106382.
33 J. Yu, Q. Guo, Y. Gong, L. Ding, J. Wang and G. Yu, *Fuel Process. Technol.*, 2021, **214**, 106723.
34 M. H. Tahir, G. Çakman, J. L. Goldfarb, Y. Topcu, S. R. Naqvi and S. Ceylan, *Bioresour. Technol.*, 2019, **279**, 67–73.
35 M. H. Tahir, Z. Zhao, J. Ren, T. Rasool and S. R. Naqvi, *Biomass Bioenergy*, 2019, **122**, 193–201.
36 S. Gupta, G. K. Gupta and M. K. Mondal, *Biomass Convers. Biorefin.*, 2022, **12**, 4847–4861.
37 T. Raj, M. Kapoor, R. Gaur, J. Christopher, B. Lamba, D. K. Tuli and R. Kumar, *Energy Fuels*, 2015, **29**, 3111–3118.
38 M. S. Ahmad, M. A. Mehmood, O. S. Al Ayed, G. Ye, H. Luo, M. Ibrahim, U. Rashid, I. Arbi Nehdi and G. Qadir, *Bioresour. Technol.*, 2017, **224**, 708–713.
39 M. H. Tahir, R. M. Irfan, X. Cheng, M. S. Ahmad, M. Jamil, T. U. H. Shah, A. Karim, R. Ashraf and M. Haroon, *J. Anal. Appl. Pyrolysis*, 2021, **155**, 105066.
40 C. S. Fermanelli, A. Córdoba, L. B. Pierella and C. Saux, *Waste Manage.*, 2020, **102**, 362–370.
41 A. Demirbaş, *Energy Sources*, 2002, **24**, 215–221.
42 P. E. A. Debiagi, C. Pecchi, G. Gentile, A. Frassoldati, A. Cuoci, T. Faravelli and E. Ranzi, *Energy Fuels*, 2015, **29**, 6544–6555.
43 W. Jerzak, A. Bieniek and A. Magdziarz, *Int. J. Hydrogen Energy*, 2021, **48**, 11680–11694.
44 M. H. Rahman, P. R. Bhoi, A. Saha, V. Patil and S. Adhikari, *Energy*, 2021, **225**, 120231.
45 A. Ahmed, M. S. Abu Bakar, R. Hamdani, Y. K. Park, S. S. Lam, R. S. Sukri, M. Hussain, K. Majeed, N. Phusunti, F. Jamil and M. Aslam, *Environ. Res.*, 2020, **186**, 109596.
46 H. Huang, J. Liu, H. Liu, F. Evrendilek and M. Buyukada, *Energy Convers. Manage.*, 2020, **207**, 112552.
47 T. A. Vo, Q. K. Tran, H. V. Ly, B. Kwon, H. T. Hwang, J. Kim and S. S. Kim, *J. Anal. Appl. Pyrolysis*, 2022, **163**, 105464.
48 D. T. Sekyere, J. Zhang, Y. Chen, Y. Huang, M. Wang, J. Wang, N. Niwamanya, A. Barigye and Y. Tian, *Fuel*, 2023, **333**, 126339.
49 H. Cai, Z. Ba, K. Yang, Q. Zhang, K. Zhao and S. Gu, *Results Phys.*, 2017, **7**, 3230–3235.
50 C. Li Nishu, D. Yellezuome, Y. Li and R. Liu, *Renew Energy*, 2023, **209**, 569–580.

51 H. Bi, C. Wang, Q. Lin, X. Jiang, C. Jiang and L. Bao, *Sci. Total Environ.*, 2021, **751**, 142293.
52 B. Lin, J. Zhou, Q. Qin, X. Song and Z. Luo, *J. Anal. Appl. Pyrolysis*, 2019, **144**, 104718.
53 H. C. Ong, W. H. Chen, Y. Singh, Y. Y. Gan, C. Y. Chen and P. L. Show, *Energy Convers. Manage.*, 2020, **209**, 112634.
54 M. A. Mehmood, G. Ye, H. Luo, C. Liu, S. Malik, I. Afzal, J. Xu and M. S. Ahmad, *Bioresour. Technol.*, 2017, **228**, 18–24.
55 D. Singh, S. Chandra and R. Pandey, *New J. Chem.*, 2023, 8022–8031.
56 Z. H. Jabbar and B. H. Graimed, *J. Water Process Eng.*, 2022, **47**, 102671.
57 Q. L. Li, R. Shan, W. J. Li, S. X. Wang, H. R. Yuan and Y. Chen, *Int. J. Hydrogen Energy*, 2024, **55**, 1476–1485.
58 M. Žula, M. Grilc and B. Likozar, *Chem. Eng. J.*, 2022, **444**, 136564.
59 H. Tian, R. Zhu, L. Chen, J. Wang and Y. Cheng, *Ind. Crops Prod.*, 2023, **204**, 117314.
60 S. R. Naqvi, A. H. Khoja, I. Ali, M. Naqvi, T. Noor, A. Ahmad, R. Luque and N. A. S. Amin, *Fuel*, 2023, **333**, 126268.
61 A. Eschenbacher, R. J. Varghese, M. S. Abbas-Abadi and K. M. Van Geem, *Chem. Eng. J.*, 2022, **428**, 132087.
62 S. Wang, Y. Sun, R. Shan, J. Gu, T. Huhe, X. Ling, H. Yuan and Y. Chen, *Int. J. Hydrogen Energy*, 2023, **48**, 23821–23830.